Binding of Antibacterial Magainin Peptides to Electrically Neutral Membranes: Thermodynamics and Structure†

Torsten Wieprecht,‡ Michael Beyermann,§ and Joachim Seelig*,‡

Department of Biophysical Chemistry, Biocenter of the University of Basel, Klingelbergstrasse 70, CH-4056 Basel, Switzerland, and Institute of Molecular Pharmacology, Alfred-Kowalke Strasse 4, D-10315 Berlin, Germany

Received April 22, 1999; Revised Manuscript Received June 7, 1999

ABSTRACT: Magainins are positively charged amphiphatic peptides which permeabilize cell membranes and display antimicrobial activity. They are usually thought to bind specifically to anionic lipids, and binding studies have been performed almost exclusively with negatively charged membranes. Here we demonstrate that binding of magainins to neutral membranes, a reaction which is difficult to assess with spectroscopic means, can be followed with high accuracy using isothermal titration calorimetry. The binding mechanism can be described by a surface partition equilibrium after correcting for electrostatic repulsion by means of the Gouy−Chapman theory. Unusual thermodynamic parameters are observed for the binding process. (i) The three magainin analogues that were investigated bind to neutral membranes with large exothermic reaction enthalpies ΔH of −15 to −18 kcal/mol (at 30 °C). (ii) The reaction enthalpies increase with increasing temperature, leading to a large positive heat capacity ΔC_p of ≈130 cal mol^{-1} K^{-1} (at 25 °C). (iii) The Gibbs free energies of binding ΔG are between −6.4 and −8.6 kcal/mol, resulting in a large negative binding entropy ΔS. The binding of magainin to small unilamellar vesicles is hence an enthalpy-driven reaction. The negative ΔH and ΔS and the large positive ΔC_p contradict the conventional understanding of the hydrophobic effect. CD experiments reveal that the membrane-bound fraction of magainin is ∼80% helical at 8 °C, decreasing to ∼60% at 45 °C. Since the random coil → α-helix transition in aqueous solution is known to be an exothermic process, the same process occurring at the membrane surface is shown to account for up to 65% of the measured reaction enthalpy. In addition to membrane-facilitated helix formation, the second main driving force for membrane binding is the insertion of the nonpolar amino acid side chains into the lipid bilayer. It also contributes a negative ΔH and follows the pattern for the nonclassical hydrophobic effect. Addition of cholesterol drastically reduces the extent of peptide binding and reveals an enthalpy−entropy compensation mechanism. Membrane permeability was measured with a dye assay and correlated with the extent of peptide binding. The level of dye efflux is linearly related to the amount of surface-bound peptide and can be traced back to a membrane perturbation effect.

Magainins are a group of antibacterial peptides isolated from the skin of the African clawed frog *Xenopus laevis* (*1*). The peptides consist of 21−23 amino acid residues, have a net positive charge, and exert their antimicrobial activity by permeabilizing the biological membrane (*2*, *3*). Peptide binding to the membrane surface is accompanied by a random coil → α-helix transition (*4*−*6*). Magainins produce membrane permeabilization by physical interaction with the bilayer itself. Experimental evidence exists both for the formation of short-lived or long-lived transmembrane pores and for a perturbation of the lipid packing (*7*−*9*). Several studies of the binding of magainin peptides to model membranes have been reported (*4*, *5*, *10*, *11*). It was shown that the peptides have a high affinity for negatively charged membranes which decreases with decreasing content of negatively charged lipids (*4*). Electrostatic interactions between the cationic magainins and anionic lipids have therefore been suggested to play a specific role in inducing membrane permeability and to be mainly responsible for the selective action of magainins at negatively charged bacterial membranes. In contrast to bacterial membranes, most eukaryotic membranes, such as the plasma membrane of human erythrocytes, do not contain negatively charged lipids in the outer leaflet. To understand the mechanism of action and to evaluate the pharmaceutical potential of magainins, it is necessary to obtain insight into the interaction of magainins also with electrically neutral membranes. Using spectroscopic techniques, magainin analogues were found to bind to neutral membranes (*4*, *12*) with partition constants similar to those observed for medium chain alcohols (*13*) or small hydrophobic peptides (*14*, *15*). However, no quantitative determination of the thermodynamics of magainin interaction with neutral phospholipids has as yet been performed since the spectroscopic effects were generally too small to allow a sufficiently precise evaluation of the binding isotherm.

† Supported by Swiss National Science Foundation Grant 31.42058.94.

* To whom correspondence should be addressed: Department of Biophysical Chemistry, Biocenter of the University of Basel, Klingelbergstrasse 70, CH-4056 Basel, Switzerland. Telephone: +41-61-267-2190. Fax: +41-61-267-2189. E-mail: seelig1@ubaclu.unibas.ch.

‡ Biocenter of the University of Basel.

§ Institute of Molecular Pharmacology.

10.1021/bi990913+ CCC: $18.00
Published on Web 07/23/1999

We have previously demonstrated that isothermal titration calorimetry is highly sensitive in detecting the binding of magainin to negatively charged membranes (*11*). We have now applied the same method to systematically investigate the thermodynamics of magainin binding or adsorption to electrically neutral, sonicated vesicles composed of 1-palmitoyl-2-oleoyl-*sn*-glycero-3-phosphocholine (POPC)[1] containing up to 40 mol % cholesterol. Analysis of the calorimetric traces as a function of the peptide and lipid concentration yielded the reaction enthalpy, ΔH, and the binding isotherms. The isotherms were analyzed in terms of a surface partition equilibrium, modulated by electrostatic interactions, providing the partition constant K, the Gibbs free energy of the reaction, ΔG, and, in turn, the entropy change, ΔS. CD measurements and dye efflux measurements were performed in parallel, and the thermodynamic data could be correlated with changes in the peptide conformation and with the induction of membrane permeability. The titrations were repeated at different temperatures, and thus, the specific heat capacity, ΔC_p, of the binding reaction could be determined. The thermodynamic results contradict the classical picture of hydrophobic interactions, and an alternative mechanism based on the coil → helix transition and the nonclassical hydrophobic effect is proposed.

MATERIALS AND METHODS

Materials. 1-Palmitoyl-2-oleoyl-*sn*-glycero-3-phosphocholine (POPC) was purchased from Avanti Polar Lipids, Inc. (Alabaster, AL). The Fmoc amino acids for peptide synthesis were obtained from Novabiochem (Bad Soden, Germany). All other chemicals were of analytical or reagent grade. Buffer was prepared from 18 MΩ water obtained from a NANOpure A filtration system.

Peptide Synthesis. Peptides were synthesized by solid-phase methods using standard Fmoc chemistry on Tenta Gel S RAM resin (0.21 mmol/g; RAPP Polymere, Tübingen, Germany) in the continuous-flow mode on a MilliGen 9050 (Millipore) peptide synthesizer (*16*). Purification was carried out by preparative high-performance liquied chromatography (HPLC) on PolyEncap A300 (10 μm, 250 mm × 20 mm inside diameter) (Bischoff Analyzentechnik GmbH, Leonberg, Germany) to give final products that were >95% pure as determined by HPLC analysis. All peptides were characterized by matrix-assisted laser desorption ionization mass spectrometry (MALDI II; Kratos, Manchester, U.K.) with the peptide content of lyophilized samples being determined by quantitative amino acid analysis (LC 3000, Biotronik-Eppendorf).

Preparation of Lipid Vesicles. A defined amount of lipid in chloroform was first dried under a nitrogen stream. To remove traces of ethanol which is frequently used to stabilize chloroform, the lipid was dissolved in dichloromethane and then again dried under nitrogen and subsequently overnight under high vacuum. Typically, 2−3 mL of buffer [10 mM Tris and 100 mM NaCl (pH 7.4)] was added to the lipid, and the dispersion was extensively vortexed. For preparation of small unilamellar vesicles (SUVs), the lipid dispersion was sonified (at 10 °C, under nitrogen) using a titanium tip ultrasonicator until the solution became transparent (about 60 min). Titanium debris was removed by centrifugation (Eppendorf tabletop centrifuge, 10 min at 14 000 rpm). The lipid concentration was calculated on basis of the weight of the dried lipid. Large unilamellar vesicles (LUVs) for dye release experiments were prepared by the extrusion method (*17*). After the dried lipid had been vortexed in calcein buffer [70 mM calcein and 10 mM Tris (pH 7.4)], the suspension was frozen and thawed in liquid nitrogen (six times) and extruded through polycarbonate filters (six times through two stacked 0.4 μm pore size filters, followed by eight times through two stacked 0.1 μm filters). Untrapped calcein was removed from vesicles by gel filtration on a Sephadex G75 column [the eluent being buffer containing 10 mM Tris and 100 mM NaCl (pH 7.4)]. The lipid concentration was determined by quantitative phosphorus analysis (*18*).

High-Sensitivity Titration Calorimetry. Isothermal titration calorimetry was performed using a Microcal MC2 high-sensitivity titration calorimeter (Microcal, Norhampton, MA; for a description, see ref *19*). Solutions were degassed under vacuum prior to use. The calorimeter was calibrated electrically. The heats of dilution were determined in control experiments by injecting either peptide solution of lipid suspension into buffer. The heats of dilution were subtracted from the heats determined in the corresponding peptide−lipid binding experiments.

Circular Dichroism Measurements. CD measurements of the peptides in buffer of in the presence of lipid vesicles were carried out on a Jasco 720 spectrometer at wavelengths of 200−260 nm. Minor contributions of circular dichroism and circular differential scattering of the SUVs were eliminated by subtracting the lipid spectra of the corresponding peptide-free suspensions. The helicity of the peptides, f_h, was determined from the mean residue ellipticity [Θ] at 222 nm according to the following equation (*20*):

$$f_h = \frac{[\Theta]_{222} + 2340}{-30300} \quad (1)$$

Dye Release Experiments. Aliquots of a vesicle suspension (10−20 μL) were injected into a cuvette containing 2.5 mL of a stirred thermostated peptide solution with a defined concentration (final lipid concentration of 50 μM). Calcein release from LUVs was assessed fluorometrically by measuring the decrease in the level of self-quenching (excitation at 490 nm and emission at 520 nm) on a Jasco FP 777 spectrofluorometer. The fluorescence intensity corresponding to 100% calcein release was determined by addition of 100 μL of a 10% Triton X-100 solution.

RESULTS

The cationic magainins exhibit a strong affinity toward membranes with negatively charged lipids, whereas the binding to neutral membranes is usually considered to be rather weak. Nevertheless, an approximate binding constant was determined indirectly for the M2a-POPC system with CD spectroscopy (*4*). In the course of our studies with charged membranes (*11*), we observed that the binding of

[1] Abbreviations: M2a, magainin 2 amide; SUV, small unilamellar vesicle; POPC, 1-palmitoyl-2-oleoyl-*sn*-glycero-3-phosphocholine; POPG, 1-palmitoyl-2-oleoyl-*sn*-glycero-3-phosphoglycerol; HPLC, high-performance liquid chromatography; Tris, tris(hydroxymethyl)aminomethane; CD, circular dichroism; LUV, large unilamellar vesicle; TFE, trifluoroethanol.

Table 1: Amino Acid Sequences,[a] Mean Residue Hydrophobicity (H),[b] and Hydrophobic Moment (M)[c] of the Magainin Anologue Peptides

peptide	sequence	H	M
M2a	GIGKF LHSAK KFGKA FVGEI MNS(NH_2)	−0.0357	0.286
$I^6A^8L^{15}I^{17}$-M2a	GIGKF ***I*****H*****A***AK KFGK***L*** F***I***GEI MNS(NH_2)	0.0157	0.280
$I^6V^9W^{12}T^{15}I^{17}$-M2a	GIGKF ***I***HS***V***K K***W***GK***T*** F***I***GEI MNS(NH_2)	−0.0350	0.317

[a] The one-letter code for amino acids was used. [b] Mean residue hydrophobicities and hydrophobic moments were calculated using the Eisenberg consensus scale of hydrophobicity (*62*). [c] Hydrophobic moments were calculated assuming ideal α-helical conformations.

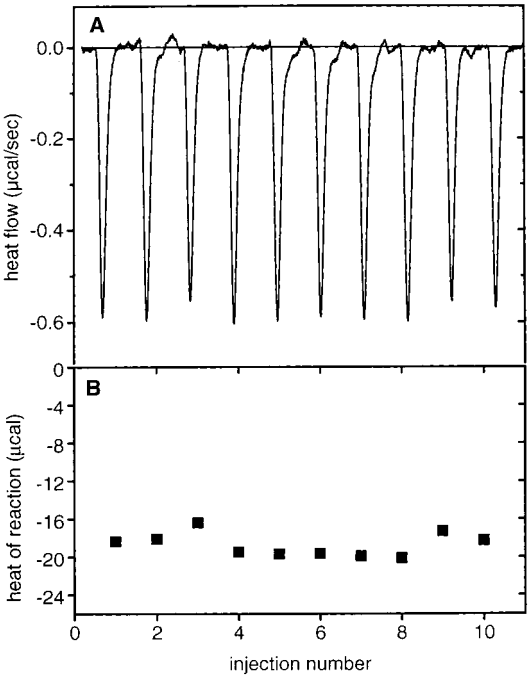

FIGURE 1: Titration calorimetry of POPC SUVs (20 mM) with a solution of M2a (200 μM) at 15 °C. Aliquots of a 5 μL peptide solution were added to the lipid suspension in the reaction cell (V = 1.3353 mL). Panel A shows the calorimeter trace. The heat of reaction as evaluated by integration of the calorimeter traces is given in panel B.

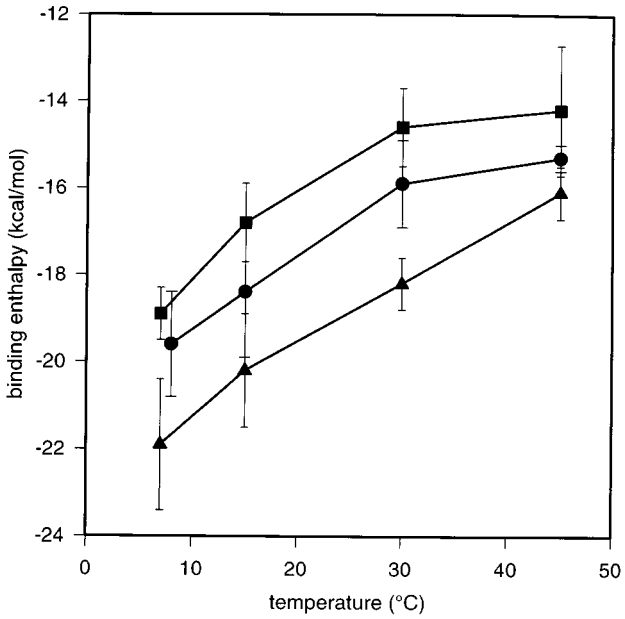

FIGURE 2: Temperature dependence of the reaction enthalpies of M2a (●), $I^6A^8L^{15}I^{17}$-M2a (■), and $I^6V^9W^{12}T^{15}I^{17}$-M2a (▲) upon binding to POPC SUVs. Binding enthalpies were calculated from titrations of POPC SUV suspensions (between 15 and 25 mM) with peptide solutions (injection of 5−6 μL of a 200 μM peptide solution).

M2a to uncharged POPC membranes is accompanied by a considerable release of heat. Isothermal titration calorimetry is thus ideally suited to analyzing the binding process. Indeed, the weak binding of magainins to neutral membranes can be measured with high accuracy and, in fact, is not as weak as usually anticipated.

The amino acid sequences of the three peptides (M2a, $I^6A^8L^{15}I^{17}$-M2a, and $I^6V^9W^{12}T^{15}I^{17}$-M2a) that were investigated are summarized in Table 1. All peptides consist of 23 amino acids and have the same total charge z of 3 (four Lys^+ and one Glu^-). In addition, the N-terminus is also partially charged at pH 7.4 (pK of the N-terminal amino group ∼ 7.2), whereas the C-terminus is amidated and carries no charge. Table 1 also includes the mean residue hydrophobicity and the hydrophobic moment, assuming a completely helical conformation. $I^6A^8L^{15}I^{17}$-M2a has an enhanced hydrophobicity, H, and $I^6V^9W^{12}I^{15}I^{18}$-M2a has an enhanced hydrophobic moment, M, compared to the parent compound M2a (*12*, *21*).

Binding Enthalpy, ΔH, Determined via Peptide-into-Lipid Titrations. Small aliquots (5−6 μL) of a peptide solution [c^0_{pep} = 200 μM; the buffer being 10 mM Tris and 100 mM NaCl (pH 7.4)] were injected into a suspension of small unilamellar POPC vesicles with a defined lipid concentration c^0_{lip} of 15−25 mM (same buffer) contained in the calorimeter cell (V_{cell} = 1.3353 mL). After the first peptide injection, the lipid-to-peptide ratio is about 25000 and decreases to about 2500 after 10 injections. Under these experimental conditions, the lipid is always in excess over the peptide.

Figure 1 displays the results of 5 μL injections of M2a (200 μM) into POPC SUVs at 15 °C. Each injection gives rise to about the same heat of reaction h_i of ca. −18.7 ± 1.2 μcal as determined from the area underneath the calorimetric traces. Injection of the same peptide solution into buffer without lipid leads to a heat of dilution h_c of −0.5 μcal which must be subtracted. The corrected heat of reaction ($\delta h_i = h_i - h_c$) divided by the amount of injected peptide yields the heat of reaction, ΔH, provided all the peptide is completely bound to the lipid membrane. Under these experimental conditions, about 98% of the added peptide is membrane-bound (cf. below). The reaction enthalpies at 15 °C (corrected for 100% binding) are distinctly exothermic with a ΔH of −18.4 ± 1.5 kcal/mol for M2a, −16.8 ± 0.9 kcal/mol for $I^6A^8L^{15}I^{17}$-M2a, and −20.2 ± 1.3 kcal/mol for $I^6V^9W^{12}T^{15}I^{17}$-M2a (Table 2).

Analogous measurements were also taken at other temperatures, and the results are shown in Figure 2. The reaction enthalpies become less exothermic with increasing temperature, yielding a large positive heat capacity change, ΔC_p, for the transfer of the peptide from the solution to the membrane. This is a surprising result since classical hydro-

Table 2: Temperature Dependence of the Thermodynamic Parameters for the Binding of the Peptides to POPC and POPC/CHOH SUVs

	ΔH^a (kcal/mol)	K^b (M^{-1})	ΔG (kcal/mol)	$-T\Delta S$ (kcal/mol)	ΔS (cal mol^{-1} K^{-1})	$\Delta C_p{}^c$ (cal mol^{-1} K^{-1})
M2a						
8 °C	-19.6 ± 1.2	10500	−7.4	12.2	−43.4	
15 °C	-18.4 ± 1.5	7000	−7.4	11.0	−38.2	
25 °C						130
30 °C	-15.9 ± 1.0	2000	−7.0	8.9	−29.4	
45 °C	-15.3 ± 0.3	440	−6.4	8.3	−26.1	
$I^6A^8L^{15}I^{17}$-M2a						
7 °C	-18.9 ± 0.6	15500	−7.6	11.3	−40.4	
15 °C	-16.8 ± 0.9	12800	−7.7	9.1	−31.6	
25 °C						131
30 °C	-14.6 ± 0.9	7700	−7.8	6.6	−21.8	
45 °C	-14.2 ± 1.5	6000	−8.0	5.9	−18.6	
$I^6V^9W^{12}T^{15}I^{17}$-M2a						
7 °C	-21.9 ± 1.5	90000	−8.6	13.3	−47.5	
15 °C	-20.2 ± 1.3	45000	−8.4	11.8	−41.0	
25 °C						149
30 °C	-18.2 ± 0.6	20000	−8.4	9.8	−32.3	
	-11.5^d	8500^d	-7.9^d	3.6^d	-12.0^d	
	-5.6^e	1500^e	-6.8^e	-1.2^e	4.1^e	
45 °C	-16.1 ± 0.6	15200	−8.6	7.5	−23.6	

[a] ΔH values are directly measured binding enthalpies estimated from peptide-into-lipid titrations; 5−6 μL of 200 μM peptide solutions was typically injected into 15−25 mM POPC SUVs in buffer [10 mM Tris and 100 mM NaCl (pH 7.4)]. [b] Binding constants were derived from lipid-into-peptide titrations using the model described in the text. Free energies and entropies were calculated using the equations $\Delta G = -RT \ln 55.5K$ and $\Delta G = \Delta H - T\Delta S$. [c] Heat capacities at 25 °C were determined from polynomial regressions of $\Delta H - T$ plots (Figure 5). [d] The membrane contains 27 mol % cholesterol. [e] The membrane contains 40 mol % cholesterol.

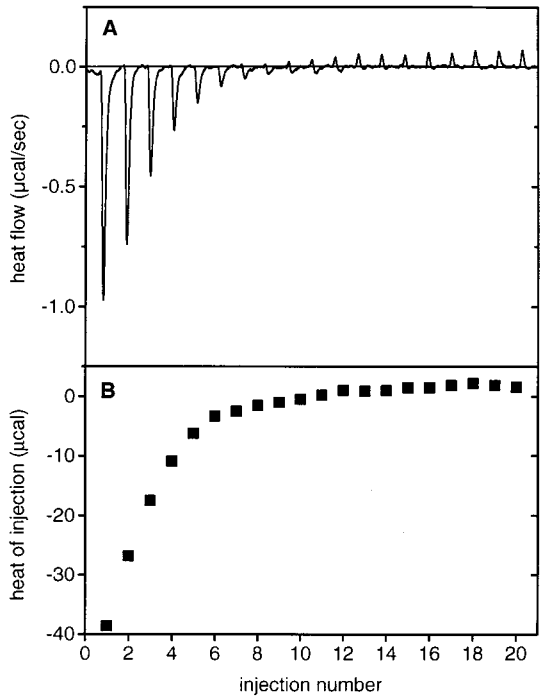

FIGURE 3: Titration calorimetry of a $I^6V^9W^{12}T^{15}I^{17}$-M2a solution (6 μM) with a POPC SUV suspension (38 mM) at 15 °C. (A) Calorimetric traces. Each peak corresponds to the injection of 5 μL of lipid suspension into the reaction cell ($V = 1.3353$ mL). (B) Heat of reaction as a function of injection number obtained by integration of the calorimeter traces. The heat of dilution was measured in a separate control experiment and was subtracted for calculation of the binding isotherm.

phobic water−oil partition processes are usually accompanied by negative ΔC_p values. For $I^6V^9W^{12}T^{15}I^{17}$-M2a (which has the largest hydrophobic moment of the three peptides), ΔH varies almost linearly between 8 and 45 °C, leading to a ΔC_p of 149 cal mol^{-1} K^{-1}. For the other two peptides, the heat capacity change is temperature-dependent and becomes smaller at higher temperatures. At 25 °C, $\Delta C_p \sim 130$ cal mol^{-1} K^{-1} for both M2a and $I^6A^8L^{15}I^{17}$-M2a and is comparable in magnitude to that of $I^6V^9W^{12}T^{15}I^{17}$-M2a.

Binding Isotherms via Lipid-into-Peptide Titrations. POPC binding isotherms were determined by injecting lipid vesicles into the peptide solution, i.e., by gradually reducing the free peptide concentration in the calorimeter cell. Results from a typical experiment are shown in Figure 3A. The calorimeter cell contained a 6 μM peptide solution ($I^6V^9W^{12}T^{15}I^{17}$-M2a) in buffer and was titrated with 5 μL aliquots of a 38 mM POPC SUV suspension. The figure demonstrates that the exothermic heat of reaction, h_i, decreases with an increasing number of injections, i, since less and less peptide is available for binding. As a control, the phospholipid suspension was injected into buffer without peptide. A constant heat of dilution h_c of $\approx$2 μcal was observed for several injections. The corrected heats of reaction ($\delta h_i = h_i - h_c$) are given in Figure 3B. δh_i approaches zero after about 15 injections, indicating that virtually all the peptide is bound to the lipid. Hence, the reaction enthalpy, ΔH, can be calculated according to

$$\Delta H = \sum_i \delta h_i / (c^0_{pep} V_{cell}) \qquad (2)$$

Next, the binding isotherm can be derived (*22*). After i injections, the fraction of peptide, $X^{(i)}_{P,b}$, bound to lipid vesicles is

$$X^{(i)}_p = \frac{n^{(i)}_{P,b}}{n^0_{pep}} = \frac{\sum_{k=1}^{i} \delta h_k}{\Delta H V_{cell} c^0_{pep}} \qquad (3)$$

where $n^{(i)}_{P,b}$ is the molar amount of bound peptide after i injections, n^0_{pep} and c^0_{pep} are the total amount and concentration, respectively, of the peptide in the calorimeter cell (cell volume V_{cell}), and $\Sigma^i_{k=1}$ δh_k is the sum of the first i reaction

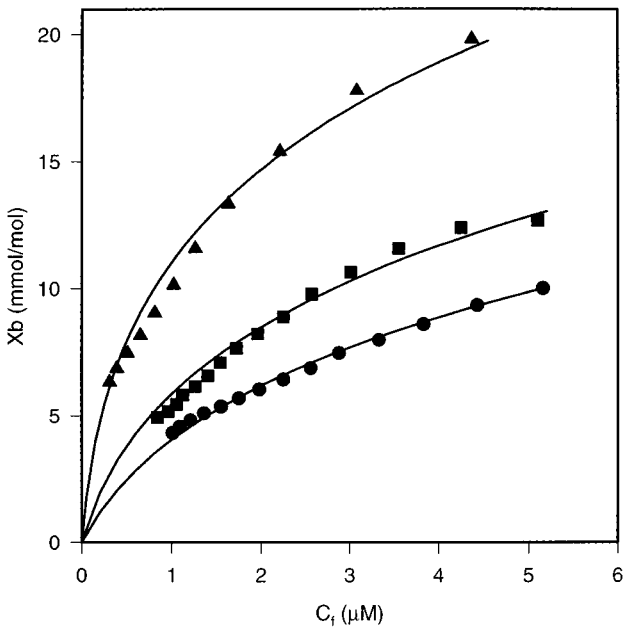

FIGURE 4: Binding isotherms for binding of magainin peptides to POPC SUVs at 15 °C: (●) M2a, (■) $I^6A^8L^{15}I^{17}$-M2a, and (▲) $I^6V^9W^{12}T^{15}I^{17}$-M2a. Binding isotherms were derived from lipid-into-peptide titrations as described in the text. The degree of binding, X_b (i.e., millimoles of peptide bound per mole of lipid in the outer lipid layer), is plotted against the free peptide concentration in bulk solution, c_f. The solid lines correspond to the theoretical binding isotherms calculated by combining a surface partition equilibrium with the Gouy−Chapman theory. The binding constants used for the calculation are given in Table 2.

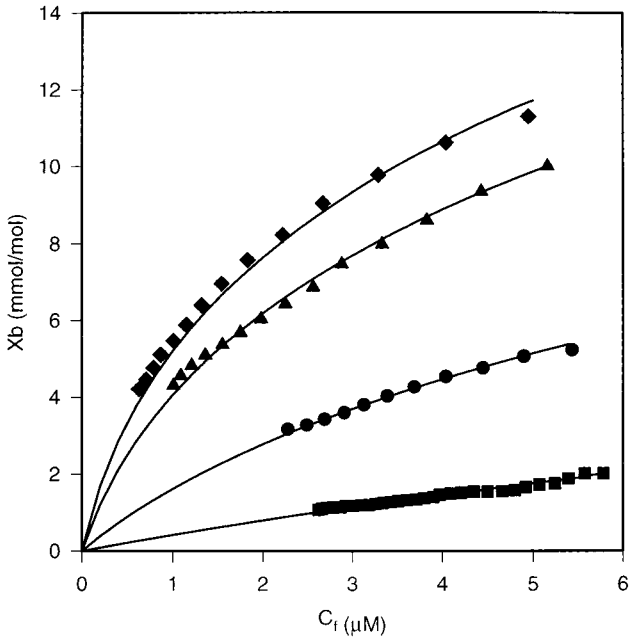

FIGURE 5: Binding isotherms for binding of M2a to POPC SUVs at different temperatures: (◆) 8, (▲) 15, (●) 30, and (■) 45 °C. Isotherms were derived from lipid-into-peptide titrations as described in the text. The degree of binding, X_b (i.e., millimoles of peptide bound per mole of lipid in the outer lipid layer), is plotted against the free peptide concentration in bulk solution, c_f. The solid lines correspond to the theoretical binding isotherms calculated by combining a surface partition equilibrium with the Gouy−Chapman theory. The binding constants used for the calculations are given in Table 2.

heats. The concentration of peptide, $c_f^{(i)}$, remaining free in solution is

$$c_f^{(i)} = f_{dil}^{(i)} c_{pep}^0 [1 - X_p^{(i)}] \quad (4)$$

The dilution factor takes into account the increase in volume due to vesicle injection and is defined as

$$f_{dil}^{(i)} = \left(\frac{V_{cell}}{V_{cell} + V_{inj}}\right)^i \approx \frac{V_{cell}}{V_{cell} + iV_{inj}} \quad (5)$$

where V_{inj} is the injected volume per injection step ($V_{inj}/V_{cell} \ll 1$). The degree of peptide binding, $X_b^{(i)}$, is defined as the fraction of bound peptide per mole of total lipid in the calorimeter cell. Since the lipid content increases with the number of injections, $X_b^{(i)}$ is given by

$$X_b^{(i)} = \frac{n_{pep,b}^{(i)}}{n_L^{(i)}} = X_p^{(i)} \frac{c_{pep}^0 V_{cell}}{iV_{inj} c_L^0} \quad (6)$$

where c_L^0 is the concentration of stock solution in the injection syringe. A plot of $X_b^{(i)}$ versus $c_f^{(i)}$ finally yields the desired binding isotherm; i.e., $X_b = f(c_f)$. It should be noted that no assumptions about the molecular nature of the binding or adsorption process must be made to derive the binding or adsorption isotherm from ITC measurements.

Figure 4 compares binding isotherms of the three different peptides measured at the same temperature of 15 °C. For the calculation of the binding isotherms, only the lipid in the outer layer of the lipid vesicles (60% of the total lipid) was considered since the highly charged peptide cannot cross the bilayer membrane at the concentrations that were employed. M2a exhibits the weakest and $I^6V^9W^{12}T^{15}I^{17}$-M2a the strongest binding. At a peptide equilibrium concentration c_f of 3 μM, the extent of $I^6V^9W^{12}T^{15}I^{17}$-M2a binding is larger by about a factor of 3 than the extent of M2a binding. The solid lines in Figure 4 correspond to calculated binding isotherms using the Gouy−Chapman theory (cf. below). The binding enthalpies, ΔH, derived from these measurements were found to be consistent with those obtained by peptide-into-lipid titrations reported in Table 2.

Finally, the influence of temperature on the binding isotherms was also measured for all three peptides, and the results for M2a are displayed in Figure 5. Peptide binding is best at low temperatures, and decreases rapidly with increasing temperatures. At a peptide equilibrium concentration c_f of 3 μM, the extent of binding decreases by about a factor of 20 between 8 and 45 °C, in agreement with the large negative reaction enthalpy of M2a.

Previous studies with M2a, using negatively charged lipids (3:1 POPC/POPG), revealed a second thermodynamic process which was tentatively assigned to M2a pore formation and pore disintegration (*11*). This process was observed at high peptide concentrations where the degree of peptide binding X_b was ≥20 mmol/mol. Such large X_b values are difficult to reach for M2a with neutral membranes. We have thus performed titration experiments with $I^6V^9W^{12}T^{15}I^{17}$-M2a, the peptide with the highest lipid affinity, at total peptide concentrations of 20 and 30 μM. Qualitatively, the same behavior was observed as for the M2a-POPC/POPG system, but the additional endothermic reaction was less pronounced than that found with negatively charged lipids.

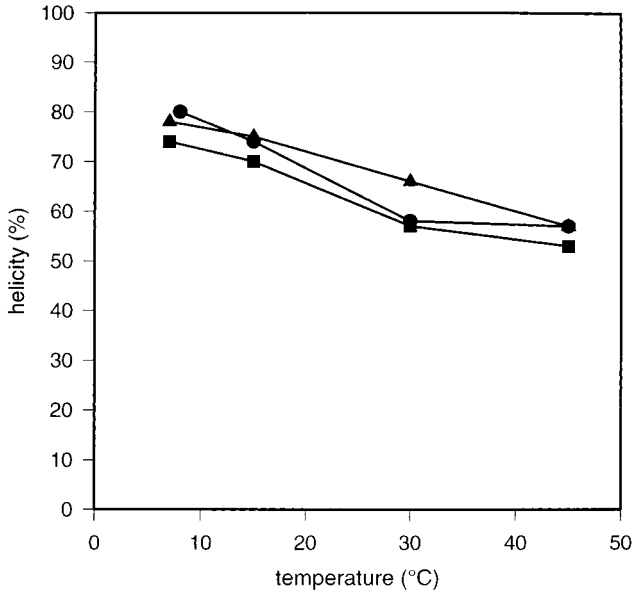

FIGURE 6: Variation of the helix content of the membrane-bound peptide fraction as a function of temperature: (●) M2a, (■) $I^6A^8L^{15}I^{17}$-M2a, and (▲) $I^6V^9W^{12}T^{15}I^{17}$-M2a.

Conformation of Membrane-Bound Magainins. The three peptides that were investigated adopt a nonordered structure in aqueous solution but become helical upon binding to the lipid membrane (*12*, *21*). Helix formation is an exothermic process with the release of −0.9 to −1.3 kcal per mole of residue (in aqueous solution) converted from random coil to α-helix (*23*−*25*). To estimate its contribution to the measured reaction enthalpy, both the extent of peptide binding and the degree of helix formation must be known. We have therefore recorded CD spectra of all three peptides in excess of POPC vesicles as a function of temperature.

The spectra are characterized by the helix double minima at 208 and 222 nm (spectra not shown). Increasing the temperature decreases the negative residual ellipticity. This is most pronounced for M2a where the apparent helix content decreases from ∼77% at 8 °C to 34% at 45 °C. In contrast, the helix content of $I^6V^9W^{12}T^{15}I^{17}$-M2a changes only from 77 to 55% in the same temperature interval. The above numbers follow from a direct evaluation of the CD spectra, and neglect the different extent of peptide binding. They represent the helix content calculated on the basis of the total peptide concentration. Knowledge of the binding isotherms of the three lipids allows the calculation of the amount of bound peptide and of the helix content of the lipid-bound peptide only. The result of this evaluation is shown in Figure 6 where the fractional helix content of the lipid-bound peptides is given as a function of temperature. The figure demonstrates that (i) all three peptides have about the same helix content when bound to the lipid vesicle and (ii) the helix content decreases linearly from ∼80% at 8 °C to ∼60% at 45 °C, corresponding to an unwinding of the helix with increasing temperature. This change in helix content will make a distinctly positive contribution to ΔC_p (cf. below).

Efflux Measurements. Magainins act by enhancing the membrane permeability, and dye leakage measurements have been reported for M2a and its two analogues (*12*, *21*). However, the earlier measurements were performed with a different salt content and in the presence of an osmotic gradient, leading to vesicle swelling. We have therefore repeated these measurements with 100 mM NaCl under isoosmolar conditions. One hundred nanometer LUVs were prepared with POPC using the polycarbonate filter method. The inside solution was 10 mM Tris and 70 mM calcein (pH 7.4); the outside solution, after gel filtration, was 10 mM Tris and 100 mM NaCl (pH 7.4). The addition of peptide induces dye leakage which is reflected in an increase of fluorescence. Figure 7A shows the extent of fluorescence dequenching, measured 5 min after addition of peptide, as a function of the total peptide concentration.

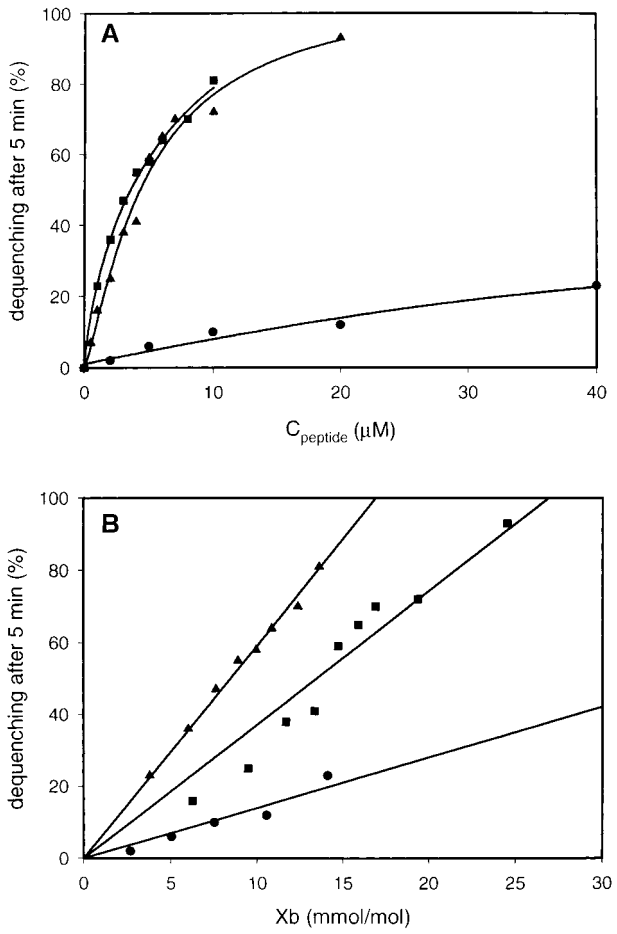

FIGURE 7: (A) Dependence of the rate of calcein leakage from POPC LUVs (given as percent dequenching after 5 min) on the total peptide concentration in solution at 30 °C. The lipid concentration was 50 μM. (B) Relationship between the rate of calcein leakage and the molar ratio of bound peptide per lipid, X_b, as calculated by combining the binding isotherms (Figures 4 and 5 and Table 2) with the results of the dye release experiments (Figure 7A): (●) M2a, (■) $I^6A^8L^{15}I^{17}$-M2a, and (▲) $I^6V^9W^{12}T^{15}I^{17}$-M2a.

By comparison of initial slopes, Figure 7 demonstrates that $I^6A^8L^{15}I^{17}$-M2a and $I^6V^9W^{12}T^{15}I^{17}$-M2a are distinctly more efficient in inducing leakage than M2a. Figure 7A reports the rate of dye efflux as a function of total peptide concentration; i.e., no distinction is made between peptide free in solution and peptide bound to the lipid vesicles. Since the binding affinities of the three peptides are different, a more relevant comparison would be to correlate the rate of dye efflux with the mole fraction of bound peptide. Such a comparison is shown in Figure 7B. It is based on a quantitative analysis of the binding isotherm and will be discussed in more detail below.

Influence of Cholesterol on Binding. Many eukaryotic membranes contain a high percentage of cholesterol, whereas

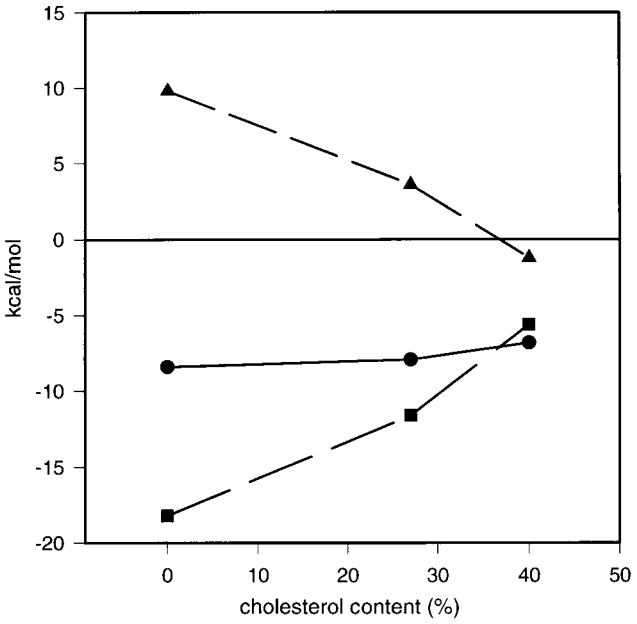

FIGURE 8: Binding of $I^6V^9W^{12}T^{15}I^{17}$-M2a to cholesterol-containing POPC SUVs at 30 °C. Dependence of the thermodynamic parameters ΔG (●), ΔH (■), and $-T\Delta S$ (▲) on cholesterol content.

bacterial membranes are generally free of cholesterol. Cholesterol was suggested to be one reason for the low lytic activity of magainins on eukaryotic membranes (*26*, *27*). Since the role of cholesterol in magainin binding has not been addressed before, we have assessed the binding of $I^6V^9W^{12}T^{15}I^{17}$-M2a (the most amphiphilic of the present peptides) to small unilamellar vesicles consisting of POPC with varying cholesterol concentrations. The ITC measurements were analyzed as described above, and the corrected binding constants were converted into free energies of binding according to the equation $\Delta G = -RT \ln 55.5K$. The thermodynamic parameters (at 30 °C) are summarized in Table 2 and in Figure 8. They are interesting for two reasons. (i) The ITC measurements demonstrate that cholesterol distinctly decreases the binding constant from 20 000 M^{-1} (no cholesterol) to 1500 M^{-1} (40% cholesterol). (ii) The POPC−cholesterol membrane is an example of an entropy−enthalpy compensation mechanism. The enthalpy, ΔH, exhibits a large variation with the cholesterol concentration and grows from about −18 kcal/mol at 0% cholesterol to about −5 kcal/mol at 40% cholesterol. Since ΔG remains approximately constant, the entropy, ΔS, which is negative at 0% cholesterol becomes positive at 40% cholesterol.

DISCUSSION

Analysis of Binding Isotherms. Hydrophobic and Electrostatic Contributions to the Binding Process. The term "binding" in the present context has a rather general meaning. In fact, the binding of magainins and other peptides to a lipid membrane is an adsorption phenomenon. No chemical bonds are formed. On the other hand, electrostatic interactions play an important role, even for noncharged membranes. As the first peptide molecules bind to the membrane, a positive surface charge develops on the outer half-layer. The adsorption of further peptides is then hindered by the repulsion of like charges. This electrostatic effect will reduce the peptide concentration near the membrane surface (denoted c_M in the following) compared to the equilibrium concentration of free peptide, c_f, in bulk solution.

The binding of the cationic magainins to electrically neutral POPC SUVs can be described by a model originally proposed for somatostatin-like peptides (*28*) and recently employed for the binding of M2a to negatively charged POPC/POPG (3:1) membranes (*11*). The model is essentially a surface partition equilibrium with the specific condition that the extent of peptide adsorption is linearly related to the peptide surface concentration, c_M (and not to the bulk concentration, c_f), i.e.

$$X_b = Kc_M \tag{7}$$

X_b has the same meaning as above, denoting the molar amount of peptide bound per mole of lipid, and K is the partition coefficient. The model has an advantage in that electrostatic effects are included in c_M. For a cationic peptide, c_M is smaller (larger) than the bulk concentration, c_f, if the membrane surface potential $\psi_0 > 0$ ($\psi_0 < 0$). c_M can be calculated from c_f and ψ_0 using the Boltzmann relation:

$$c_M = c_f \exp(-zF_0\psi_0/RT) \tag{8}$$

where z is the peptide charge, F_0 is the Faraday constant, and RT is the thermal energy. Unfortunately, the membrane potential ψ_0 cannot be measured directly. However, ψ_0 is connected with the membrane surface charge density, σ, which, in turn, is linearly related to the extent of binding X_b. The quantitative relation between σ and ψ_0 is provided by the Gouy−Chapman theory (for reviews, see refs *29*−*31*):

$$\sigma^2 = 2000\epsilon_0\epsilon_r RT\sum_i c_i(e^{-z_iF_0\psi_0/RT} - 1) \tag{9}$$

where c_i is the concentration of the ith electrolyte in the bulk aqueous phase, z_i the signed valency of the ith species, ϵ_0 the electric permittivity of free space, and ϵ_r the dielectric constant of water. Combining eqs 7−9 and calculating σ from the experimentally accessible X_b, we were then able to find a numerical solution for K, ψ_0, and c_M for each experimental data pair of X_b and c_f. The partition coefficient K ($=X_b/c_M$) describes the hydrophobic binding or adsorption process and should be independent of the peptide concentration if the model is a correct representation of the binding process.

Using this model, the experimental binding isotherms were compared with theoretical simulations. For all three peptides, a fixed charge z of 3 (four Lys and one Glu) was assumed. A pH-dependent protonation of the N-terminus was also included, assuming a pK value of 7.2 for the N-terminal amino group and calculating the pH at the membrane surface with the Gouy−Chapman theory. The solid lines in Figure 4 are the best theoretical fits to the experimental binding isotherms. An excellent agreement between theory and experiment is observed, supporting the assumption of a simple surface partition equilibrium. The partition constants according to eq 7 are 7000 M^{-1} for M2a, 12 800 M^{-1} for $I^6A^8L^{15}I^{17}$-M2a, and 45 000 M^{-1} for $I^6V^9W^{12}T^{15}I^{17}$-M2a at 15 °C (cf. Table 2).

The same approach was applied in analyzing the temperature dependence of the binding isotherms, and the solid lines

in Figure 5 are again the best theoretical fits. The partition constants and thermodynamic parameters of all the peptides that were investigated are summarized in Table 2. For M2a, the partition constant decreases from $\sim 10^4$ M^{-1} at 8 °C to 5×10^2 M^{-1} at 45 °C, consistent with the large negative ΔH.[2]

It is instructive to compare bulk properties with those encountered at the membrane surface. At a peptide bulk concentration c_f of 1 μM, a buffer pH of 7.4, and a measuring temperature of 15 °C (Figure 4), the surface concentration, c_M, of M2a ($I^6A^8L^{15}I^{17}$-M2a or $I^6V^9W^{12}T^{15}I^{17}$-M2a) decreases to 0.6 μM (0.5 and 0.2 μM, respectively), the surface potential ψ_0 equals 3.9 mV (5.6 and 10.4 mV, respectively), and the pH at the membrane surface increases to 7.5 (7.6). The apparent partition constants defined as $K_{app} = X_b/c_f$ are by a factor of 2 (M2a) to 5 ($I^6V^9W^{12}T^{15}I^{17}$-M2a) smaller than the true partition constant (at $c_f = 1$ μM). Furthermore, K_{app} is not constant but decreases with increasing peptide concentrations. The effective charge of the peptide at the membrane surface (z) is ≈3.3.

These measurements provide the first comprehensive thermodynamic analysis of the binding of antibacterial peptides to neutral membranes. In contrast to previously held views, all three peptides exhibit a considerable affinity toward uncharged bilayers which increases in the following order: M2a < $I^6A^8L^{15}I^{17}$-M2a < $I^6V^9W^{12}T^{15}I^{17}$-M2a. Surprisingly, M2a exhibits a much larger hydrophobic partition constant for neutral membranes ($K \approx 2 \times 10^3$ M^{-1}) than for negatively charged membranes ($K \sim 50$ M^{-1} at 30 °C; *11*). This suggests that the hydrophobic side chains penetrate deeper into a neutral membrane than into a negatively charged membrane. In the latter case, specific charge−charge interactions could position the peptide at a more distant layer of the surface region, maximizing the contact with the polar groups.

Knowledge of the partition constant K allows the calculation of the Gibbs free energy ΔG according to the equation $\Delta G = -RT \ln 55.5K$, where the factor 55.5 corrects for the cratic contribution to the binding (*32*). The corresponding data are summarized in Table 2. While the partition constants vary by 2 orders of magnitude (between a K of 440 M^{-1} for M2a at 45 °C and a K of 9×10^4 M^{-1} for $I^6V^9W^{12}T^{15}I^{17}$-M2a at 7 °C), the ΔG values change more modestly and fall between −6.4 and −8.6 kcal/mol. Table 2 further demonstrates that under all conditions ΔH is considerably more negative than ΔG. From the relation $\Delta G = \Delta H - T\Delta S$, it follows that the entropy ΔS is also distinctly negative (cf. Table 2). The binding of the magainins to the neutral lipid membrane is thus driven by enthalpy, whereas the entropy term counteracts binding.[3]

Small differences in the thermodynamic parameters were observed for peptides with different structural parameters. An enhanced hydrophobicity ($I^6A^8L^{15}I^{17}$-M2a) or hydrophobic moment ($I^6V^9W^{12}T^{15}I^{17}$-M2a) resulted in an increased membrane affinity. While the increased affinity of $I^6A^8L^{15}I^{17}$-M2a is caused by a reduced negative entropy, the enhanced negative ΔG for binding of $I^6V^9W^{12}T^{15}I^{17}$-M2a to POPC SUVs is a consequence of an increased negative ΔH.

Helix Formation as a Driving Force for Membrane Binding. The finding that magainin binding is driven by enthalpy but opposed by entropy must be contrasted with the classical understanding of the hydrophobic effect which is considered to be an entropy-driven process at room temperature (*33*). A nonpolar molecule is thought to partition from water into a nonpolar phase because its hydration shell is released during the transition, increasing the entropy of the system. A typical example is the transition of a hexane molecule from water into liquid hexane. The solubility of hexane in water is low because the entropy term for the transition from the aqueous phase to hexane is favorable with a $T\Delta S$ of 7.7 kcal/mol, whereas $\Delta H \approx 0$ kcal/mol (at room temperature) (*34*). A related example, relevant for membrane equilibria and measured with isothermal titration calorimetry, is the partitioning of the surfactant octylglucoside from the aqueous phase into the lipid membrane. This process is also entropy-driven with a $T\Delta S$ of 6.5 kcal/mol and counteracted by a positive enthalpy ΔH of 1.3 kcal/mol (*35*). A second characteristic feature of the hydrophobic effect is its strong dependence on temperature (*34*). Typically, the enthalpy for the transfer from water to the organic phase decreases with increasing temperature, and the molar heat capacity, ΔC_p, is distinctly negative. For example, the transfer of octylglucoside from water to the lipid membrane has a ΔC_p of ca. −75 cal K^{-1} mol^{-1} at 25 °C (*35*).

It is obvious that the binding of the magainins to neutral membranes does not follow the classical pattern of the hydrophobic effect. The unusual results are the large negative binding enthalpy (−14 to −22 kcal/mol), the negative entropy (−19 to −48 cal mol^{-1} K^{-1}), and the positive ΔC_p (∼130 cal mol^{-1} K^{-1}). In the following, we suggest that these findings are caused, in part, by the formation of an α-helix at the membrane surface.

Helix formation is an exothermic process. Calorimetric values for the enthalpy of helix formation, Δh_{helix}, have been determined for poly-L-glutamate and poly-L-lysine (−1.1 and −0.9 kcal/mol of residues, respectively) (*23*, *36*), and noncalorimetric estimates with similar magnitudes have been reported for these and other peptides (*37*). The enthalpy change for the random coil to α-helix transition has also been measured calorimetrically for a 50-residue peptide that contains primarily alanine. The transition enthalpy could be

[2] Under favorable conditions, the partition constant can be evaluated even without resorting to the Gouy−Chapman theory. This is possible for neutral membranes at very low degrees of peptide adsorption since electrostatic repulsions can then be neglected. The tangent to the adsorption isotherm at the origin will yield the true partition constant K. The data depicted in Figures 4 and 5 were analyzed by this approach and were found to be in approximate agreement with the more accurate Gouy−Chapman analysis.

[3] We have also measured the extent of binding of $I^6V^9W^{12}T^{15}I^{18}$-M2a to 100 nm unilamellar vesicles (LUVs) prepared by extrusion. In accordance with previous studies (*39*), binding to POPC LUVs is less exothermic ($\Delta H \sim -5$ kcal/mol at 30 °C) than binding to POPC SUVs (−18.2 kcal/mol). Because of the reduced binding enthalpy and the comparably weak affinity for electrically neutral membranes, a reliable determination of a binding isotherm was not possible by means of ITC. However, we have compared binding of M2a to POPC/POPG (3:1) SUVs and LUVs (T. Wieprecht and J. Seelig, manuscript in preparation) and found only minor differences in the binding constants between LUVs and SUVs but again a large difference in ΔH (−3 kcal/mol for LUVs and −17 kcal/mol for SUVs). If we assume that the free energy of binding of $I^6V^9W^{12}T^{15}I^{18}$-M2a to POPC LUVs is largely unchanged compared to that to SUVs, the enthalpy term is still the dominating contribution to the negative free energy. Therefore, the conclusion drawn in the following parts of the discussion section should be valid also for binding of magainins to large vesicles.

determined only within broad limits (−0.9 kcal/mol of residues > Δh_{helix} > −1.3 kcal/mol of residues) (*25*). Finally, the human plasma apolipoproteins, apo-A-II and apo-C−III, were found to associate with phospholipid with a concurrent increase in α-helical structure, and an exothermic helix formation enthalpy Δh_{helix} of −1.3 kcal/mol of residues was deduced (*24*). Helix induction in trifluoroethanol (TFE)/water mixtures was studied with CD spectroscopy and led to a considerably smaller enthalpy Δh_{helix} of −0.7 kcal/mol of residues with 35% TFE (*38*). Since TFE/H_2O mixtures are often considered membrane-mimicking solvents, the latter value represents the extreme for a helix inserted into the nonpolar part of the membrane.

It is now possible to estimate the contribution of α-helix formation to the enthalpy of magainin association with the lipid membrane. If a Δh_{helix} of −0.7 kcal/mol of residues and M2a with a helix content of ∼80% at 8 °C are chosen (Figure 6), helix formation should contribute −12.9 kcal/mol (experimental value of −19.6 kcal/mol). At 45 °C, the M2a helix content is reduced to ∼60% and the calculated transition enthalpy decreases concomitantly to −9.7 kcal/mol (experimental value of −15.2 kcal/mol). Similar results were obtained for $I^6A^8L^{15}I^{17}$-M2a and $I^6V^9W^{12}T^{15}I^{17}$-M2a. With the Δh_{helix} parameter characteristic of hydrophobic solvents, helix formation at the membrane surface would account for 65% (M2a and $I^6A^8L^{15}I^{17}$-M2a) to 55% ($I^6V^9W^{12}T^{15}I^{17}$-M2a) of the total enthalpy (*28*, *39*). It can hence be concluded that membrane-facilitated helix formation is a strong driving force for magainin binding to the lipid membrane.

Side Chain Penetration as a Nonclassical Hydrophobic Effect. Using lipid photolabels, magainin side chains have been detected to insert deeply into the lipid bilayer (*40*). Side chain penetration into SUVs has been found to be an exothermic reaction, at least for a series of somatostatin-like peptides (*28*, *39*). The enthalpic component is also dominant in membrane-binding reactions of many hydrophobic cations and anions with quite different chemical structures (*41*, *42*), contradicting the traditional view of the hydrophobic effect that the transfer enthalpy for a nonpolar substance from water into the membrane should be close to zero at room temperature. This "nonclassical" hydrophobic effect (*41*, *43*) is not limited to membrane systems but may also be found for tight apolar inclusion compounds (*44*, *45*). For the magainins investigated here, side chain insertion contributes between −5 and −10 kcal/mol (i.e., $\Delta H_{exp} - \Delta H_{helix}$) to the binding process. This magnitude is similar to that observed for the binding of somatostatin analogues which like the magainins have two phenylalanine side chains on the same side of the cyclic structure (*28*, *39*). It is hence suggested that side chain insertion, in particular Phe insertion, follows the nonclassical hydrophobic effect and is the second main driving force for magainin binding.

In a related study, the binding of apolipoprotein A-I model compounds (with a chain length similar to that of magainin) to POPC vesicles was studied with isothermal titration calorimetry and spectroscopic methods (*46*, *47*). The change in helix content upon lipid binding was less dramatic ($\Delta f_{helix} \approx 16-48\%$) compared to that of the magainins. However, the reaction enthalpy was also distinctly exothermic for all peptides investigated with ΔH values in the range of −4.2 to −11.2 kcal/mol. Twenty-six to seventy-five percent of the total ΔH was due to helix formation, and the rest must again be assigned to a nonclassical hydrophobic effect (*46*, *47*).

An Unusual Heat Capacity ΔC_p. Both the classical and nonclassical hydrophobic effect are characterized by a negative heat capacity change, ΔC_p, for the transfer of a nonpolar molecule from water to the organic phase. In the traditional picture, the hydrophobic surface leads to the formation of "structured water", sometimes called "iceberg". The large negative ΔC_p is then thought to be caused by the loss of the iceberg as the molecule enters the hydrophobic phase (*48*).

The unusual experimental result in this study is the large positive ΔC_p of ∼130 cal mol^{-1} K^{-1} (at 25 °C) for magainin binding which, in fact, constitutes the first observation of this kind in membrane partitioning equilibria. A partial explanation for a positive ΔC_p is the melting of the membrane-bound α-helix. From the enthalpies given above, this contribution to ΔC_p can be estimated to be 87 cal mol^{-1} K^{-1} for M2a. It should be offset, in part, by the negative ΔC_p of the side chain penetration. However, even in the absence of the latter effect, the heat capacity of helix melting would still be too small to explain the experimental observation of ΔC_p of 130 cal mol^{-1} K^{-1}. At present, one can only spectulate about additional mechanisms that lead to the large ΔC_p. One possibility would be a perturbation of the lipid membrane in a manner such that a larger hydrophobic surface area becomes exposed to water. The net effect of magainin insertion would thus be an increase in the size of the iceberg. Indirect support for such a mechanism is given by the increased leakiness of the lipid membrane upon peptide binding (cf. below). In addition, the fatty acyl chain of the phospholipids could adopt a more disordered conformation. Liquid-like hydrocarbon chains have a higher molar heat capacity than ordered chains. Finally, it should be pointed out that the transfer of polar amino acids from water to the nonpolar environment also has a positive ΔC_p (*48*, *49*). Hence, if some polar residues of the magainin peptides are forced into a nonpolar environment, this could also lead to an increase in ΔC_p.

Comparison with Negatively Charged Membranes. Previous studies of magainin binding to lipid membranes have relied on spectroscopic techniques such as fluorescence or CD spectroscopy using negatively charged membranes. No distinction was made between electrostatic and hydrophobic binding, and the binding process was described by an overall binding constant. A much larger apparent binding constant was observed for negatively charged than for neutral membranes, and it was concluded that magainin peptides bind specifically to negatively charged membranes. This conclusion must be modified in the light of the results presented here. Magainins have a high affinity toward negatively charged membranes because the peptide accumulates in the aqueous lipid−water interface by electrostatic attraction, and not because it binds specifically to anionic lipids. The binding step proper, i.e., the transition from the interfacial layer with its high magainin concentration, c_M, to the membrane surface, has a low binding constant [$K = 50$ M^{-1} (*11*)]. Indeed, in the hypothetical case in which the concentration gradient near the membrane surface could be eliminated, magainins would bind distinctly better to neutral than to charged membranes.

Magainin Binding and Membrane Permeability. Magainins are biologically important because they permeabilize membranes for ions (*2*, *3*, *50*). Structural models have been proposed in which magainins insert into the membrane and form a transmembrane pore or channel (*10*, *51*−*54*). In one model, the pore exists only as a short-lived intermediate (*2*, *3*, *10*, *52*−*54*); in the second, a stable structure that can be detected with neutron diffraction experiments at high magainin concentrations has been elucidated (*55*, *56*). In a third model, on the basis of NMR experiments, the peptide does not cross the membrane but remains associated in helical form parallel to the membrane surface (*6*, *57*−*59*). In this orientation, leakiness must be induced by a lipid perturbation mechanism. Pore formation and lipid perturbation thus appear to be alternative pathways by which magainins permebilize membranes.

The dye efflux shown in Figure 7 follows the lipid perturbation model. First, the binding isotherms can only be explained if the peptides are assumed to remain on the outside of the vesicles. Second, the rate of dye efflux correlates linearly with the amount of surface-bound peptide even at the lowest peptide concentration. In Figure 7A, the rate of dye release is plotted as a function of total peptide concentration, c^0_{pep}. Knowledge of the binding isotherms allows a calculation of the concentration of free peptide, c_f, and of the amount of bound peptide, X_b, under the same experimental conditions. Figure 7B then shows the rate of dye efflux as a function of the degree of binding, X_b. This representation eliminates the influence of the different peptide binding affinities. Within the accuracy of the measurements, straight lines through the origin are obtained for all three peptides that were investigated. No threshold values and no evidence for magainin aggregation or association can be deduced from these results. This does not support a pore formation mechanism (with a critical number of magainins lining the pore) for the specific systems that were investigated.

As an aside, it can be noted that in addition to the binding affinity the chemical nature of the peptide has a specific impact on the dye efflux. This follows from the different slopes in Figure 7B. Since binding effects are eliminated in this representation, the slopes are a direct measurement of peptide efficiency. Inspection of the slopes reveals that $I^6A^8L^{15}I^{17}$-M2a ($I^6V^9W^{12}T^{15}I^{17}$-M2a) is by a factor of 4.2 (2.6) more efficient in inducing dye release than M2a. This finding together with the enhanced lipid affinity of these analogues is in agreement with the increased hemolytic activity of $I^6V^9W^{12}T^{15}I^{17}$-M2a and $I^6A^8L^{15}I^{17}$-M2a compared to that of M2a (*12*, *21*).

Influence of Cholesterol. Cholesterol was previously shown to reduce the lytic activity of magainin peptides (*26*, *27*). However, the reasons for the activity reduction were unknown. Our results show that addition of cholesterol reduces the binding constant of $I^6V^9W^{12}T^{15}I^{17}$-M2a from 20 000 M^{-1} (0% cholesterol) to 1500 M^{-1} (40% cholesterol). For a given peptide concentration, c_f, the amount of magainin bound to a 40% cholesterol-containing membrane is only 10% of that observed for a cholesterol-free membrane. This suggests that the reduced membrane affinity is a major reason for the activity reduction in the presence of cholesterol.

From the thermodynamic point of view, addition of cholesterol is accompanied by a relatively moderate increase in ΔG, but by a large increase in ΔH and a corresponding increase in $T\Delta S$ (Figure 8), indicating an enthalpy−entropy compensation mechanism. Enthalpy−entropy compensation mechanisms have been found for other hydrophobic systems such as cylophane-arene (*45*) or cyclodextrin inclusion compounds (*44*, *60*, *61*) and are difficult to explain in molecular terms. In the case presented here, a partial explanation can be provided by a combination of two effects. First, the incorporation of cholesterol leads to an increase in vesicle size. The binding enthalpy of hydrophobic substances to lipid vesicles is known to depend on the vesicle size; for small vesicles, ΔH is generally very exothermic ($\Delta H \ll 0$), but with increasing vesicle size, ΔH grows and can assume even positive values (*25*, *39*, *47*). Second, cholesterol is known to induce an ordering of the lipid acyl chains and to enhance the lipid packing density. Therefore, the potential of peptide to enhance van der Waals interactions between lipid acyl chains and to induce acyl chain ordering on membrane binding is expected to be reduced in already well-ordered and tightly packed cholesterol−lipid bilayers. In agreement with the experimental observations, the presence of cholesterol should result in a reduced negative enthalpy contribution (or even in a positive enthalpy contribution) from van der Waals interaction as well as in a reduced contribution to $-T\Delta S$. A similar enthalpy−entropy compensation mechanism was recently reported for the partitioning of *n*-alcohols with different chain lengths into cholesterol-free and cholesterol-containing membranes (*13*).

Concluding Remarks. Isothermal titration calorimetry combined with CD spectroscopy has provided the first comprehensive thermodynamic analysis of the binding of magainin peptides to neutral membranes. The hydrophobic binding affinity of magainins to neutral membranes is distinctly higher than that observed for negatively charged membranes. However, the additional electrostatic interaction encountered with negatively charged membranes more than compensates for the smaller hydrophobic contribution. The binding reaction is enthalpy-driven, and helix formation at the membrane surface accounts for as much as ∼65% of the total enthalpy; the rest must be attributed to the insertion of nonpolar amino acid side chains into the nonpolar part of the membrane. The large positive heat capacity change of the binding reaction is unique for magainins and does not correspond to the expectations based on simple models for the classical or nonclassical hydrophobic effect. The induction of membrane leakiness requires peptide binding to the membrane outside only and is a linear function of the amount of surface-bound peptide.

ACKNOWLEDGMENT

We thank Dr. W. L. Maloy (Magainin Pharmaceuticals, Inc., Plymouth Meeting, PA) for the generous gift of magainin 2 amide.

REFERENCES

1. Zasloff, M. (1987) *Proc. Natl. Acad. Sci. U.S.A. 84*, 5449−53.
2. Westerhoff, H. V., Juretic, D., Hendler, R. W., and Zasloff, M. (1989) *Proc. Natl. Acad. Sci. U.S.A. 86*, 6597−601.

3. Westerhoff, H. V., Hendler, R. W., Zasloff, M., and Juretic, D. (1989) *Biochim. Biophys. Acta 975*, 361−9.
4. Wieprecht, T., Dathe, M., Schumann, M., Krause, E., Beyermann, M., and Bienert, M. (1996) *Biochemistry 35*, 10844−53.
5. Matsuzaki, K., Harada, M., Funakoshi, S., Fujii, N., and Miyajima, K. (1991) *Biochim. Biophys. Acta 1063*, 162−70.
6. Bechinger, B., Zasloff, M., and Opella, S. J. (1993) *Protein Sci. 2*, 2077−84.
7. Duclohier, H., Molle, G., and Spach, G. (1989) *Biophys. J. 56*, 1017−21.
8. Grant, E., Jr., Beeler, T. J., Taylor, K. M., Gable, K., and Roseman, M. A. (1992) *Biochemistry 31*, 9912−8.
9. Matsuzaki, K., Murase, O., Fujii, N., and Miyajima, K. (1996) *Biochemistry 35*, 11361−8.
10. Matsuzaki, K., Murase, O., Tokuda, H., Funakoshi, S., Fujii, N., and Miyajima, K. (1994) *Biochemistry 33*, 3342−9.
11. Wenk, M. R., and Seelig, J. (1998) *Biochemistry 37*, 3909−16.
12. Wieprecht, T., Dathe, M., Beyermann, M., Krause, E., Maloy, W. L., MacDonald, D. L., and Bienert, M. (1997) *Biochemistry 36*, 6124−32.
13. Rowe, E. S., Zhang, F., Leung, T. W., Parr, J. S., and Guy, P. T. (1998) *Biochemistry 37*, 2430−40.
14. Jacobs, R. E., and White, S. H. (1986) *Biochemistry 25*, 2605−12.
15. Jacobs, R. E., and White, S. H. (1989) *Biochemistry 28*, 3421−37.
16. Beyermann, M., Wenschuh, H., Henklein, P., and Bienert, M. (1992) *Innovation and Perspectives in solid-phase synthesis*, Intercept Limited, Andover, MD.
17. Hope, M. J., Bally, M. B., Webb, G., and Cullis, P. R. (1985) *Biochim. Biophys. Acta 812*, 55−65.
18. Böttcher, C. J. F., van Gent, C. M., and Pries, C. (1961) *Anal. Chim. Acta 24*, 203−4.
19. Wiseman, T., Williston, S., Brandts, J. F., and Lin, L. N. (1989) *Anal. Biochem. 179*, 131−7.
20. Chen, Y. H., Yang, J. T., and Martinez, H. M. (1972) *Biochemistry 11*, 4120−31.
21. Wieprecht, T., Dathe, M., Krause, E., Beyermann, M., Maloy, W. L., MacDonald, D. L., and Bienert, M. (1997) *FEBS Lett. 417*, 135−40.
22. Seelig, J. (1997) *Biochim. Biophys. Acta 1331*, 103−16.
23. Chou, P. Y., and Scheraga, H. A. (1971) *Biopolymers 10*, 657−80.
24. Massey, J. B., Gotto, A. M., Jr., and Pownall, H. J. (1979) *J. Biol. Chem. 254*, 9559−61.
25. Scholtz, J. M., Marqusee, S., Baldwin, R. L., York, E. J., Stewart, J. M., Santoro, M., and Bolen, D. W. (1991) *Proc. Natl. Acad. Sci. U.S.A. 88*, 2854−8.
26. Tytler, E. M., Anantharamaiah, G. M., Walker, D. E., Mishra, V. K., Palgunachari, M. N., and Segrest, J. P. (1995) *Biochemistry 34*, 4393−401.
27. Matsuzaki, K., Sugishita, K., Fujii, N., and Miyajima, K. (1995) *Biochemistry 34*, 3423−9.
28. Seelig, J., Nebel, S., Ganz, P., and Bruns, C. (1993) *Biochemistry 32*, 9714−21.
29. Aveyard, R., and Haydon, D. A. (1973) *An Introduction to the Principles of Surface Chemistry*, Cambridge University Press, London.
30. McLaughlin, S. (1977) *Curr. Top. Membr. Transp. 9*, 71−144.
31. McLaughlin, S. (1989) *Annu. Rev. Biophys. Biophys. Chem. 18*, 113−36.
32. Cantor, C. R., and Schimmel, P. R. (1980) *Biophysical Chemistry*, Vol. 1, Freeman, San Francisco.
33. Tanford, F. (1980) *The hydrophobic effect: formation of micelles and biological membranes*, Wiley & Sons, New York.
34. Privalov, P. L., and Gill, S. J. (1988) *Adv. Protein Chem. 39*, 191−234.
35. Wenk, M. R., Alt, T., Seelig, A., and Seelig, J. (1997) *Biophys. J. 72*, 1719−31.
36. Rialdi, G., and Hermans, J., Jr. (1966) *J. Am. Chem. Soc. 88*, 5719−20.
37. Hermans, J., Jr. (1966) *J. Phys. Chem. 70*, 510−5.
38. Luo, P., and Baldwin, R. L. (1997) *Biochemistry 36*, 8413−21.
39. Beschiaschvili, G., and Seelig, J. (1992) *Biochemistry 31*, 10044−53.
40. Jo, E., Blazyk, J., and Boggs, J. M. (1998) *Biochemistry 37*, 13791−9.
41. Huang, C. H., and Charlton, J. P. (1972) *Biochemistry 11*, 735−40.
42. Seelig, J., and Ganz, P. (1991) *Biochemistry 30*, 9354−9.
43. Jencks, C. (1969) *R.I. Med. J. 52*, 558−62.
44. Clarke, R. J., Coates, J. H., and Lincoln, S. F. (1988) *Adv. Carbohydr. Chem. Biochem. 46*, 205−49.
45. Smithrud, D. B., Wyman, T. B., and Diederich, F. (1991) *J. Am. Chem. Soc. 113*, 5420−6.
46. Gazzara, J. A., Phillips, M. C., Lund-Katz, S., Palgunachari, M. N., Segrest, J. P., Anantharamaiah, G. M., and Snow, J. W. (1997) *J. Lipid Res. 38*, 2134−46.
47. Gazzara, J. A., Phillips, M. C., Lund-Katz, S., Palgunachari, M. N., Segrest, J. P., Anantharamaiah, G. M., Rodrigueza, W. V., and Snow, J. W. (1997) *J. Lipid Res. 38*, 2147−54.
48. Müller, N. (1992) *Trends Biochem. Sci. 17*, 459−63.
49. Spolar, R. S., Livingstone, J. R., and Record, M. T., Jr. (1992) *Biochemistry 31*, 3947−55.
50. Gomes, A. V., de Waal, A., Berden, J. A., and Westerhoff, H. V. (1993) *Biochemistry 32*, 5365−72.
51. Cruciani, R. A., Barker, J. L., Zasloff, M., Chen, H. C., and Colamonici, O. (1991) *Proc. Natl. Acad. Sci. U.S.A. 88*, 3792−6.
52. Cruciani, R. A., Barker, J. L., Durell, S. R., Raghunathan, G., Guy, H. R., Zasloff, M., and Stanley, E. F. (1992) *Eur. J. Pharmacol. 226*, 287−96.
53. Matsuzaki, K., Murase, O., and Miyajima, K. (1995) *Biochemistry 34*, 12553−9.
54. Matsuzaki, K., Murase, O., Fujii, N., and Miyajima, K. (1995) *Biochemistry 34*, 6521−6.
55. Ludtke, S. J., He, K., Wu, Y., and Huang, H. W. (1994) *Biochim. Biophys. Acta 1190*, 181−4.
56. Ludtke, S., He, K., and Huang, H. (1995) *Biochemistry 34*, 16764−9.
57. Bechinger, B., Zasloff, M., and Opella, S. J. (1992) *Biophys. J. 62*, 12−4.
58. Bechinger, B. (1997) *Proteins 27*, 481−92.
59. Hirsh, D. J., Hammer, J., Maloy, W. L., Blazyk, J., and Schaefer, J. (1996) *Biochemistry 35*, 12733−41.
60. Inoue, Y., Hakushi, T., Liu, Y., Tong, L.-H., Shen, B.-J., and Jin, D.-S. (1993) *J. Am. Chem. Soc. 115*, 475−81.
61. Zhang, B., and Breslow, R. (1993) *J. Am. Chem. Soc. 115*, 9353−4.
62. Eisenberg, D. (1984) *Annu. Rev. Biochem. 53*, 595−623.

BI990913+